Journal of Cleaner Production 208 (2019) 743–752

Contents lists available at ScienceDirect

Journal of Cleaner Production

journal homepage: www.elsevier.com/locate/jclepro

Understanding the variability of urban heat islands from local background climate and urbanization☆

Ranhao Sun [a, **], Yihe Lü [a, b], Xiaojun Yang [c], Liding Chen [a, b, *]

[a] State Key Laboratory of Urban and Regional Ecology, Research Center for Eco-Environmental Sciences, Chinese Academy of Sciences, Beijing 100085, China
[b] University of Chinese Academy of Sciences, Beijing 100049, China
[c] Department of Geography, Florida State University, Tallahassee, FL 32306, USA

A R T I C L E I N F O

Article history:
Received 13 October 2017
Received in revised form
29 September 2018
Accepted 15 October 2018
Available online 16 October 2018

Keywords:
Urban warming
Global warming
Urban green
Energy consumption
Anthropogenic heat
Urbanization

A B S T R A C T

Climate change adaptation in urban areas is among the biggest challenges humanity faces partly because of the combined effects of urban heating and global warming. The variability of urban heat islands (VUHIs) is known to influence the effectiveness of climate adaptation strategies; however, the understanding of VUHIs is still limited. Here, we quantified the diurnal and seasonal VUHIs in 245 Chinese cities that varied in population and physical size based on the remotely sensing data from 2002 to 2012. Taking the 2012 VUHIs as an example, we examined the relationships between VUHIs and underlying drivers of background climate and urbanization. The results showed that: (1) the VUHIs from 2002 to 2012 had obvious periodicity in different years while significant diurnal and seasonal variability; (2) the explanation rates of local background climate for the diurnal VUHIs were 30% (spring), 19% (summer), 29% (autumn), and 25% (winter), respectively; (3) the explanation rates of urbanization for the diurnal VUHIs were 13% (spring), 22% (summer), 11% (autumn), and 21% (winter), respectively; (4) these two variables also accounted for 32% and 12% of the seasonal VUHIs during the daytime, and 25% and 23% during the nighttime, respectively. Our research suggests that the improvement of urban climate-change adaptation necessitates local "climate-smart" strategies, a reduction in local anthropogenic heat emissions, and rational use of green planning for sustainable urban development.

1. Introduction

The combined effects of urban heating and global warming make adapting urban areas to climate change one of the biggest challenges facing humanity (Georgescu et al., 2014; Parker, 2004; Patz et al., 2005; Sun et al., 2016). The percentage of the world's population living in urban areas is increasing rapidly and expected to reach nearly 70% by 2050 (UNDESA, 2015). At the same time, the global climate continues to change at an unprecedented rate (IPCC, 2014; Parker, 2004; Sun et al., 2016). This combination makes urban areas an increasingly important component of the Earth's land surface (Lee and Kim, 2016). Accordingly, there is an urgent need to integrate environmental management and the design and planning of energy systems (Theodosiou et al., 2015).

The sensible and latent heat fluxes in urbanized regions can be altered by changes in land-surface properties, leading to the urban heat island (UHI) phenomenon which is characterized by temperature difference between urban and surrounding rural areas. Over the years, various efforts have been made to examine UHI intensity (Peng et al., 2012; Schwarz et al., 2011; Zhao et al., 2014), footprints (Zhou et al., 2015), and potential causes (Li et al., 2017a; Peng et al., 2016; Stone et al., 2013; Zhou et al., 2014). The UHI phenomenon is one of the most well-established human-induced environmental impacts, and determining how to mitigate the risk of extreme heat in urban areas has been the subject of much research (Fischer and Schar, 2010; Georgescu et al., 2014; Gunawardena et al., 2017; Ramamurthy and Bou-Zeid, 2017; Stone et al., 2013). Recent studies have shown that changes in land-surface heat fluxes and local anthropogenic heat emissions can produce variability in the strength of UHIs over time (Sailor et al., 2015; Steeneveld et al., 2014; Zhang et al., 2013), and this variability exacerbates the consequences of global climate change (Fischer and Schar, 2010) by

☆ The authors are willing to share the dataset in Excel format with those who wish to replicate the results of this study.

* Corresponding author. State Key Laboratory of Urban and Regional Ecology, Research Center for Eco-Environmental Sciences, Chinese Academy of Sciences, Beijing 100085, China.
** Corresponding author.
E-mail addresses: rhsun@rcees.ac.cn (R. Sun), liding@rcees.ac.cn (L. Chen).

https://doi.org/10.1016/j.jclepro.2018.10.178
0959-6526/

disrupting vegetation growth (Li et al., 2017b; Zhao et al., 2016), raising energy consumption for heating and cooling (Zhang et al., 2013), and affecting residents' health (Patz et al., 2005; Youngsteadt et al., 2017).

Although controversy persists regarding the impact of urban warming on global climate change and extreme climatic events (Fischer and Knutti, 2015; Gaffin et al., 2012), the synergistic interactions between UHIs and extreme heat events have been well recognized in some cities (Fischer and Schar, 2010; Ramamurthy and Bou-Zeid, 2017). Ongoing large-scale research has revealed the spatial distribution of the UHIs of selected megacities (Estoque et al., 2017), including 32 in China (Zhou et al., 2014), 18 in Asia (Huang et al., 2006), 38 in the United States (Imhoff et al., 2010), and 65 in North America (Zhao et al., 2014). Understanding the variability of UHIs (VUHIs) might help quantify contributions to global climate change; however, VUHIs remain poorly understood over large areas. Moreover, few studies have systematically analyzed VUHIs and their underlying drivers (Zhou et al., 2014). Therefore, it is not clear if VUHIs have diurnal and seasonal differences or what factors contribute significantly to this variability. In particular, we believe closer attention to a broader spectrum of cities with various climates and degrees of urbanization is urgently needed. Accordingly, a quantitative understanding of VUHIs would help policymakers formulate appropriate climate change adaptation strategies in an increasingly urbanizing world.

China has diverse climate types and has experienced rapid urbanization in recent decades (Cao et al., 2016b). The level of urbanization can affect the contribution of urban heat to global warming (Sun et al., 2016; Zhou et al., 2004). Remote sensing data is well suited to providing large-scale observations of land surface temperatures which are highly correlated with air temperatures (Clinton and Gong, 2013). Therefore, for this study, the UHI intensity and variability were examined in 245 Chinese cities from 2002 to 2012 using observations of the Moderate Resolution Imaging Spectroradiometer (MODIS). Moreover, we used the climate and urbanization data in 2012 to correlate the day-night and summer-winter VUHIs with underlying factors.

2. Materials and methods

2.1. Remotely sensed and statistical datasets

Cities have been growing rapidly in China and their natural boundaries are more meaningful than administrative boundaries when assessing the UHI intensity in different years. Urban boundaries in this study were extracted from nighttime satellite images from 2002 to 2012 using a single-pixel-value cutoff. This cutoff is a hierarchical classification based on the head/tail breaks of city size (Jiang et al., 2015). Using this method, we obtained the natural urban footprints of 245 Chinese cities from 2002 to 2012. Rural areas were defined as being within the buffer zone around the urban area, covering the same amount of land as the urban area.

The contributions of anthropogenic heat can be calculated by separately considering the major sources of waste heat generated in urban environments from energy, vehicles, and human metabolism individually (Sailor et al., 2015; Sun et al., 2018). This study used energy consumption, vehicle, and population data for the 245 Chinese cities available in the *China City Statistical Yearbook 2012*, *China Energy Statistical Yearbook 2012*, and *Statistical Yearbook Series of China 2012*. The local background climate was assessed by precipitation, air temperature, and wind. We collected the raster data of monthly precipitation, monthly air temperature, and monthly wind velocity from the China Meteorological Data Sharing Service System. This dataset has been verified with comprehensive checking of temporal and internal consistency, evaluation of biases and long-term drifts of sensors and modules, malfunction of sensors, etc. The data describing the local background climate has a 1000 m spatial resolution. We used the mean value of local background climate within the urban area of each city. The relative elevation of each city was then quantified by differences in the elevation between urban and rural areas.

The Moderate Resolution Imaging Spectroradiometer (MODIS) data set was provided by the Geospatial Data Cloud site, Computer Network Information Center, Chinese Academy of Sciences. Aqua land surface temperature data were obtained from 2002 to 2012 for the 245 cities (examples in 2012 see Supplementary Figs 1 & 2). This is a monthly clear-sky composite dataset with a spatial resolution of 500 m. The satellite overpass times were approximately 0130 and 1330 local time, which are close to the times of daily minimum and maximum temperature. The monthly normalized difference vegetation index (NDVI) in 2012 was calculated from the near infrared and red bands of the MODIS images with a spatial resolution of 500 m (see Supplementary Fig. 3). The urban-rural NDVI difference was calculated using the mean NDVI values for the urban and rural areas.

2.2. UHI intensity and variability

The UHI intensity (I) was calculated as the difference in land surface temperature between urban (T_{urban}) and rural areas (T_{rural}):

$$I = T_{urban} - T_{rural} \tag{1}$$

We averaged daytime and nighttime UHI intensity in four seasons to examine diurnal and seasonal variability for spring (March–May), summer (June–August), autumn (September–November), and winter (December–February). The diurnal VUHI (DV) was defined as the daily range of UHI while the seasonal VUHI during daytime (SV_{day}) and nighttime (SV_{night}) were defined as the range of UHI between summer and winter:

$$\mathrm{DV} = I_{day} - I_{night} \tag{2}$$

$$SV_{day} = I_{day}^{summer} - I_{day}^{winter} \tag{3}$$

$$SV_{night} = I_{night}^{summer} - I_{night}^{winter} \tag{4}$$

2.3. Multivariate regression models

Stepwise regression methods can be easily managed and are widely used in finding key factors associated with a single dependent variable (Huang and Townshend, 2003; Ji and Chen, 2017; Kolasa-Wiecek, 2015; Yamashita et al., 2007). Compared with other complex nonlinear models, we can quantify the relative contributions of each independent variable to the total explanations using linear regression models. Here we used the linear stepwise regression method to quantify the correlations between the VUHIs and potential indicators (Supplementary Table 1):

$$V = \alpha_1 P + \alpha_2 T + \alpha_3 W + \alpha_4 H + \alpha_5 N + \alpha_6 E + \alpha_7 R + \alpha_8 C + \varepsilon \tag{5}$$

where V represents the diurnal and seasonal VUHIs; α_1 … α_1 represent the regression coefficients for independent variables; P represents monthly precipitation (mm); T represents monthly air temperature (°C); W represents monthly wind (m/s); H represents relative elevation (m); N represents relative NDVI (N); E represents the energy consumption (10^6 TCE - ton of standard coal equivalent);

R represents the resident population (10^6); C represents the domestic vehicles (10^4); and ε is the random disturbance.

The determination coefficient (R^2) and adjusted determination coefficient (Adj_R^2) were used to represent the explanation rate of the model. The contribution of each indicator to the VUHIs was quantified by its independent explanation rate derived from multiple regression. The contribution of local background climate to the VUHIs was assessed using a city's seasonal precipitation, seasonal air temperature, seasonal wind velocity, and relative elevation between the urban and rural areas. The impact of urbanization on the VUHIs was combined using the urban population, energy consumption, vehicle quantity, and relative NDVI between the urban and rural areas. The Durbin-Watson (*DW*) value is a test statistic for detecting the presence of autocorrelation in residuals. A *DW* value of 2 indicates no autocorrelation.

3. Results

3.1. Annual periodicity of VUHIs

Urban areas of Chinese cities expanded rapidly from 2002 to 2012. The total area of 245 cities increased from 41,600 km^2 in 2002 to 138,700 km^2 in 2012 (Fig. 1). The urban expansion led to differences of VUHIs in different years (Fig. 2). Compared with the annual periodicity of VUHIs, the diurnal and seasonal VUHIs were particularly significant during these years. Specifically, the daytime UHI intensity was highest in summer, followed by spring, autumn, and winter. In contrast, the UHI intensity during nighttime had less variability in different seasons. The daytime UHI intensity was higher than the nighttime UHI intensity in summer while it was lower in winter and autumn. These results showed that UHIs occurred more frequently during nighttime than daytime. In this study, we used the data of energy, vehicles, population, and climate in 245 cities to identify the underlying drivers of VUHIs. We just collected the data in 2012 due to the data availability. Therefore, we selected the 2012 VUHIs as an example to quantify the diurnal and seasonal VUHIs associated with potential drivers.

3.2. Diurnal and seasonal VUHIs

The VUHI histogram in 2012 showed that the amount and intensity of DV changed across four seasons (Fig. 3). The proportion of cities with a positive DV accounted for 62% of the total cities in spring, 72% in summer, 52% in autumn, and 29% in winter. The mean DV intensity of the 245 cities for each of the four seasons beginning with spring was 0.15 °C, 0.5 °C, −0.04 °C, and −0.53 °C, respectively. The SV histogram showed significant differences between daytime and nighttime. Among all cities, 91% had a positive SV during daytime while only 57% experienced a positive SV at nighttime (Fig. 3). The mean SV intensity was 1.25 °C during daytime and 0.13 °C at night. The DV and SV values showed a certain large-scale geographical pattern. Cities located in southeastern China exhibited a higher DV than those in the north and northwest (Fig. 4), while cities in northern China experienced a higher daytime SV but lower nighttime SV. Moreover, we noted that highly urbanized regions occupied higher DV and SV values, such as the Yangtze Delta and Pearl River Delta (Fig. 4). For example, the mean DV value for each of the four seasons beginning with spring was 1.6 °C, 1.59 °C, 1.0 °C, and 0.99 °C in the Yangtze Delta. The mean SV value in this region was 1.38 °C and 0.74 °C during daytime and nighttime, respectively.

3.3. Predication models of VUHIs

We developed predication models for the DV in different seasons and SV during daytime and nighttime. The models based on the local background climate and urbanization together accounted for 40−47% of the DV and SV (Table 1; Fig. 5). The factors influencing local background climate included precipitation, air temperature, wind, and relative elevation of the urban areas. The precipitation and air temperature had positive effects on the DV and SV, while wind had a negative influence. The high elevation of urban areas can increase the DV in spring while it will decrease the DV in winter and SV during nighttime. The factors of urbanization included urban population, vehicle quantity, energy consumption, and relative values of NDVI between the urban and rural regions. The energy and vehicle had positive effects on the DV and SV, while the NDVI had negative effects. The urban population only had negative effects on the DV in winter.

The relative contributions of potential drivers can be quantified by the standard coefficient of regression models (Fig. 6). The explanation rates of local background climate for the DV were 30% (spring), 19% (summer), 29% (autumn), and 25% (winter), respectively. The explanation rates of urbanization for the DV were 13% (spring), 22% (summer), 11% (autumn), and 21% (winter), respectively. These two variables also accounted for 32% and 12% of the seasonal VUHIs during the daytime, and 25% and 23% during the nighttime, respectively. The results showed that urban green spaces served as temperature regulators to mitigate DV in spring, summer and autumn as well as the daytime SV. However, this service was negligible in winter DV and nighttime SV when vegetation activity (e.g., latent heat flux) is relatively low. Moreover, the contribution of urban green spaces to UHI mitigation was limited, ranging from 5% in autumn to 13% in spring. In contrast, the vehicle quantity can explain 15% of the summer DV while the energy consumption had the same explanation rate for winter DV. The total explanation rates of anthropogenic heat emissions (i.e., energy and vehicle) reached 9% in the daytime SV and 17% in the nighttime SV, respectively. The intensive use of energy and vehicles should be the reason for high DV and SV values in urban agglomeration regions of China.

4. Discussion

4.1. Potential drivers of VUHIs

Current references were mainly focused on the UHI intensity itself at different times and seasons. This study investigated the variability of UHIs between day and night as well as summer and winter. The results of our study indicated that local background climate played an important role in the VUHIs. The physical mechanism of local background climate can be explained by the evapotranspiration capability in different regions and seasons. Local background climate can lead to differences in evapotranspiration over large areas (Zhao et al., 2014). Indeed, even when the urban-rural difference in vegetation cover was the same, the greater evapotranspiration produced a higher daytime UHI and lower nighttime UHI intensity, and thus high DV. Cities in southern and southeastern China had higher urban-rural differences in evapotranspiration than dry cities in northwestern China. Similarly, cities in northern China had larger summer-winter differences in air temperature and humidity than southern cities, leading to large differences in daytime evapotranspiration and high SV. Moreover, the high wind velocity can strengthen air exchange between urban and rural regions and thus lower DV and SV. The findings from this study supported the arguments about the importance of local background climate in previous studies (Peng et al., 2012; Zhao et al., 2014; Zhou et al., 2014). Annual-mean precipitation had important effect on the temporal sensitivity of UHIs in the US cities (Zhao et al., 2014) and Chinese cities (Zhou et al., 2016). A previous

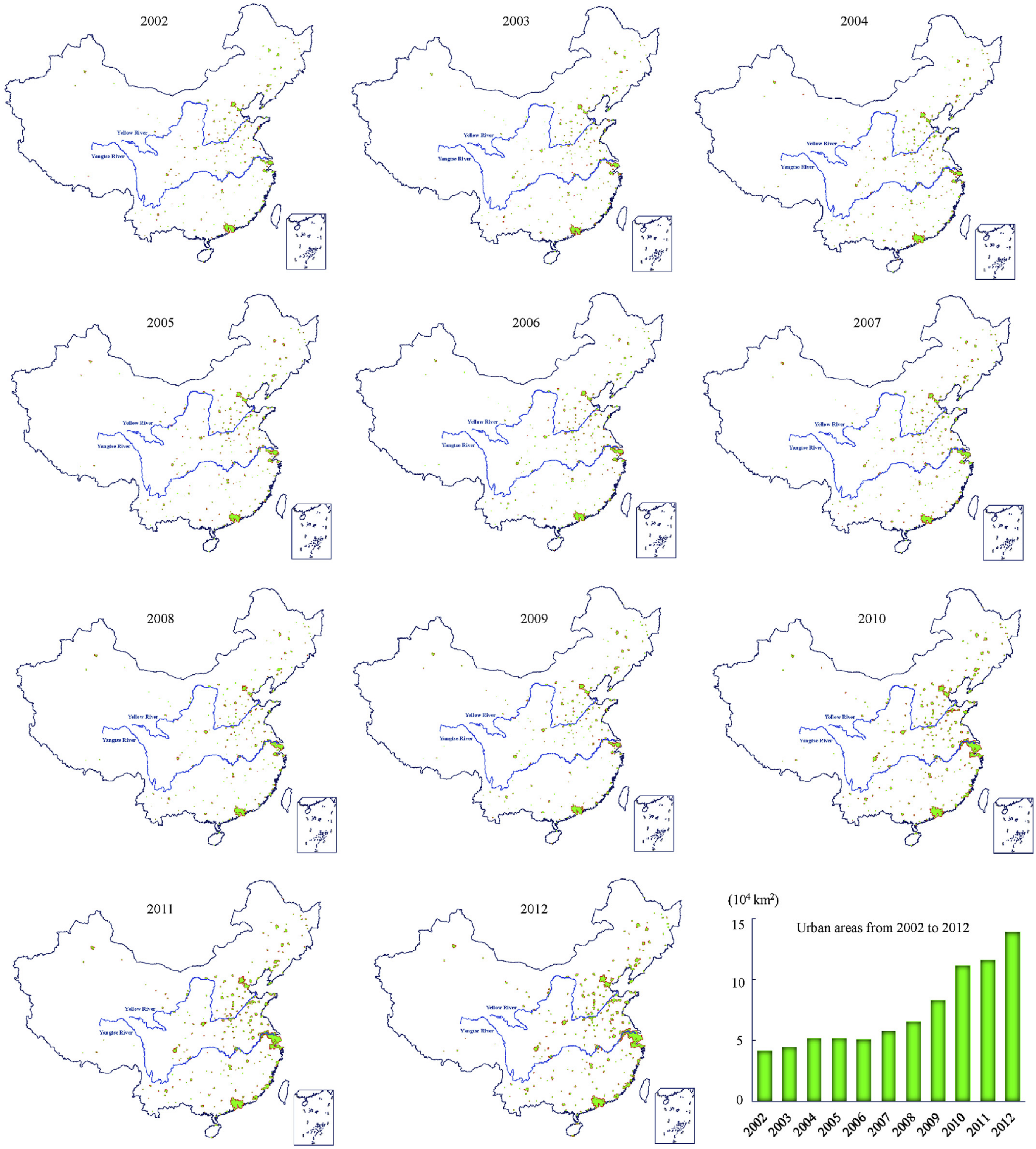

Fig. 1. The urbanization of 245 Chinese cities from 2002 to 2012. Green patches indicate urban regions and red patches indicate the rural regions. A rural area was defined as a region within the buffer zone around the urban area, covering the same amount of land as the urban area. (For interpretation of the references to colour in this figure legend, the reader is referred to the Web version of this article.)

study also found that vegetation had greatest effect on UHIs in northern China while electricity and vehicle use were important factors in southern China (Wang et al., 2015). Another research in different climate zones exhibited the contributions of local background climate to the cooling effect of urban green vegetation (Yu et al., 2018). Unlike previous studies using geographic location, this study quantified the local background climate based on seasonal precipitation, seasonal temperature, and seasonal wind. We

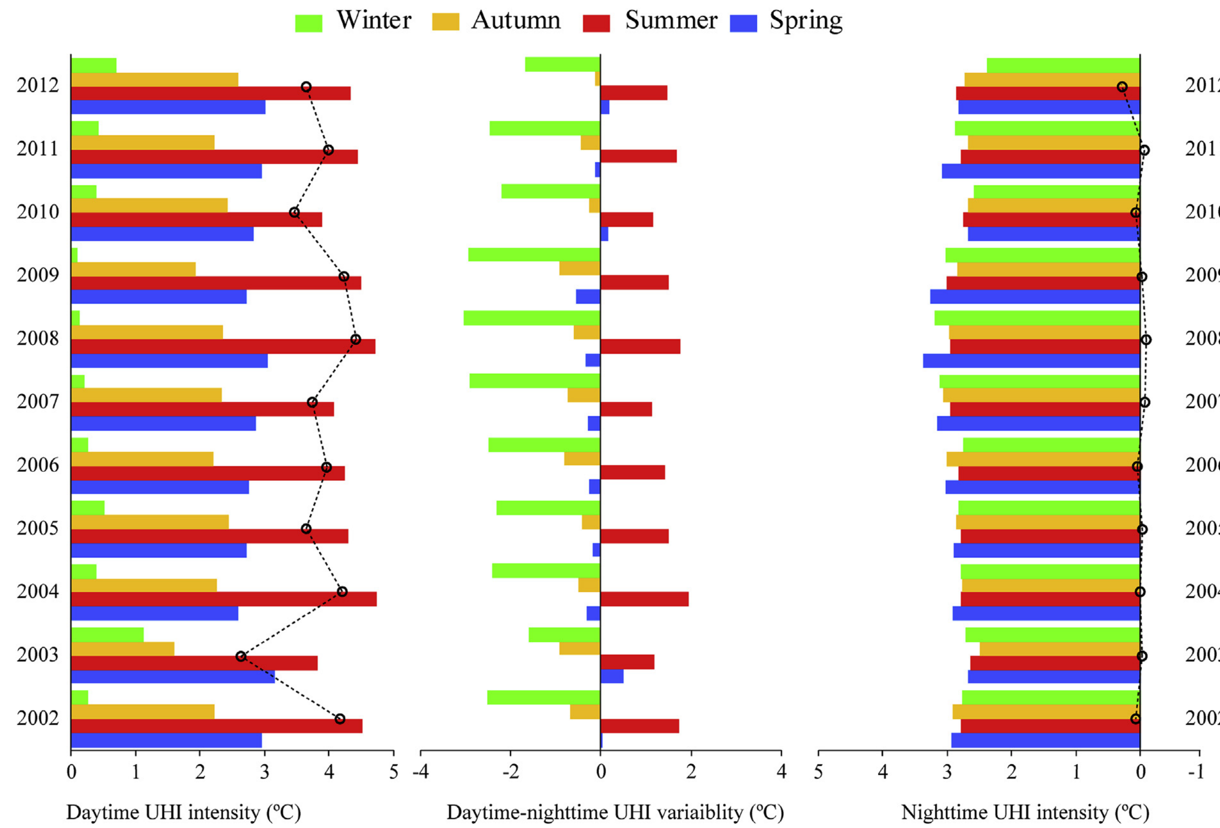

Fig. 2. Remotely-sensed urban heat island (UHI) intensity in 245 Chinese cities in daytime (a) and nighttime (b). The UHI intensity is the average of 245 cities in four seasons. The black dashed-lines show the summer-winter variability of UHI intensity in each year.

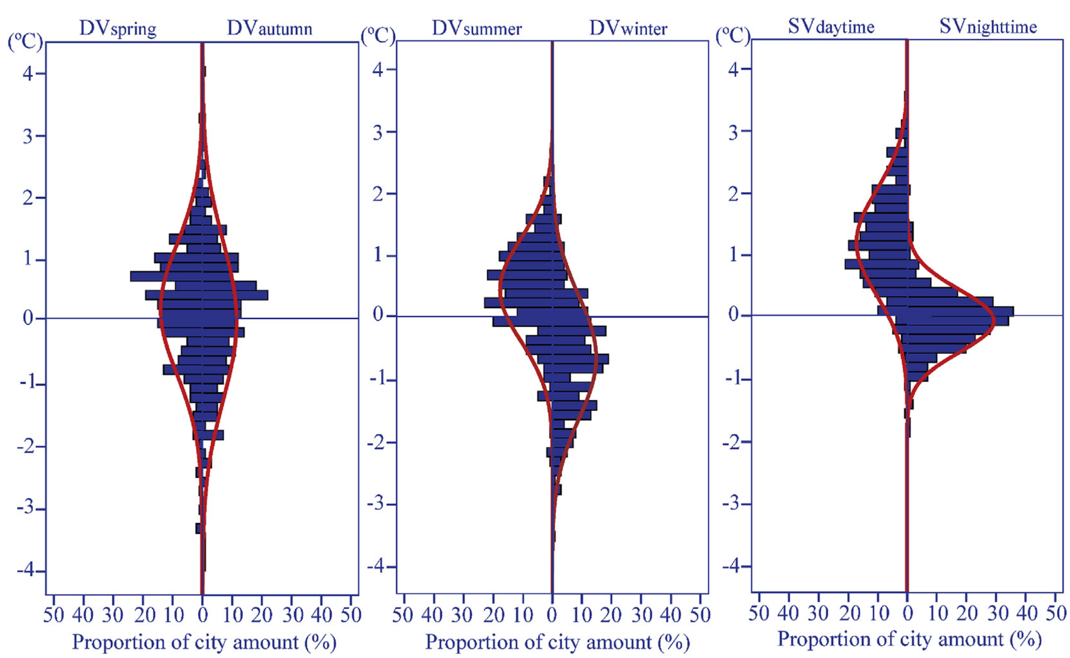

Fig. 3. Proportion of cities, and the diurnal and seasonal variability of urban heat islands in 2012. The histogram of diurnal variability of urban heat islands (DV) is similar between spring and autumn but is almost the opposite between summer and winter. Most cities (93%) experience positive summer-winter variability (SV) during daytime while only 60% show positive SV in the nighttime. The red lines show the normal distribution curves fitted to the histogram data. (For interpretation of the references to colour in this figure legend, the reader is referred to the Web version of this article.)

therefore quantified the specific contributions of influencing factors to the variability of UHIs in different seasons.

The physical mechanism of urbanization to the DV and SV depended on the seasonal variation in anthropogenic heat

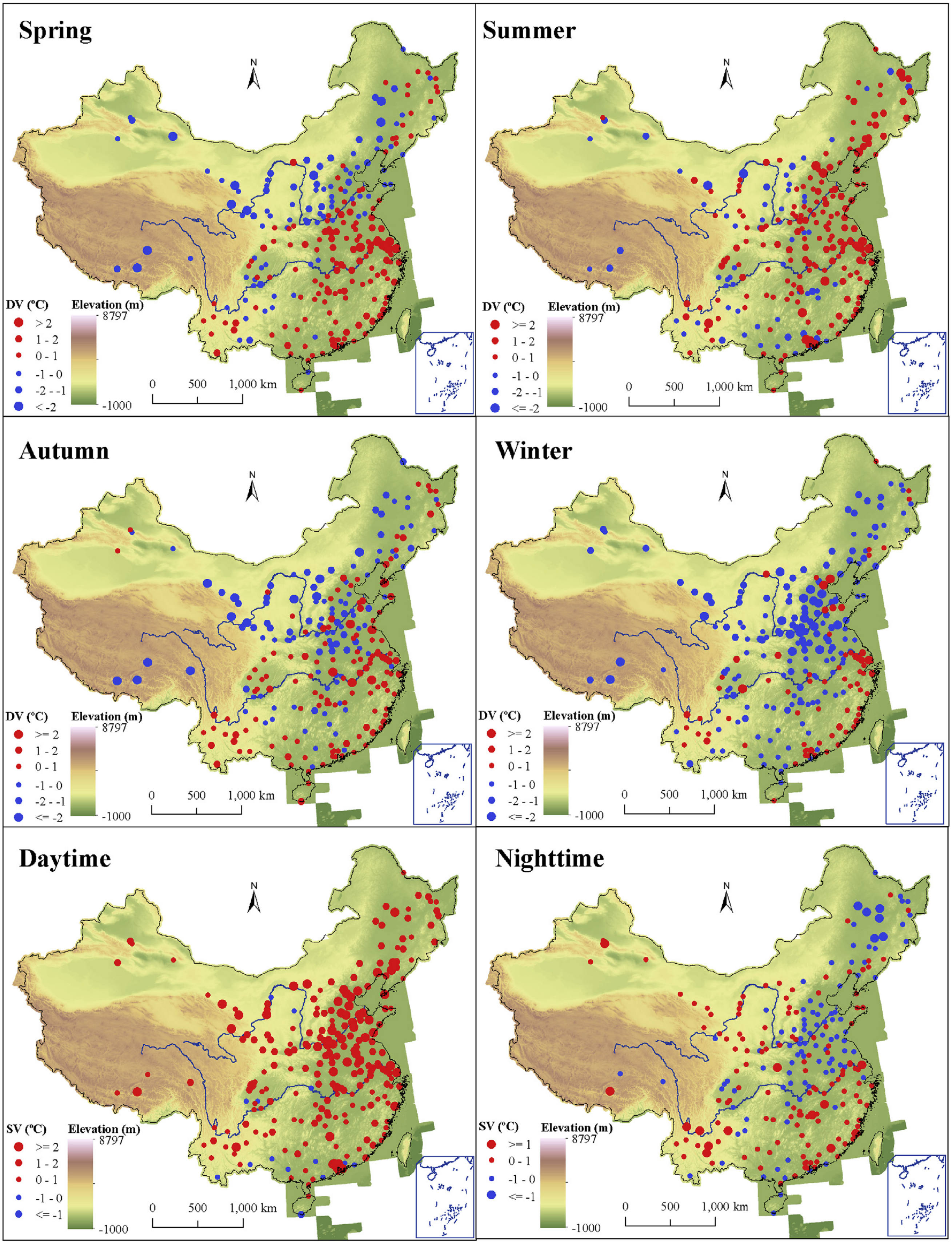

Fig. 4. Spatial distribution of diurnal and seasonal variability of urban heat islands in 245 Chinese cities in 2012. The diurnal variability (DV) maps show the day-night variability of urban heat islands in spring, summer, autumn, and winter. The seasonal variability (SV) maps indicate the summer-winter variability in the daytime and nighttime.

Table 1
Model equations of diurnal (DV) and seasonal (SV) variability of urban heat islands. R^2, determination coefficient; Adj_R^2, adjusted determination coefficient; DW, Durbin-Watson value; F, statistical significance of the model; P, precipitation; T, air temperature; W, wind velocity; E, energy consumption; R, resident population; C, domestic vehicles; H, differences in elevation between urban and rural areas; N, differences in vegetation index between urban and rural areas.

	Regression Model	R^2	Adj_R^2	F ($p < 0.01$)	DW
DV_{spring}	$V = 0.375 + 0.044\ T_{spring} - 4.05\ W_{spring} + 0.004\ H - 4.5\ N_{spring}$	0.434	0.425	46.02	1.57
DV_{summer}	$V = -0.859 + 0.056\ T_{summer} - 0.273\ W_{summer} - 3.393\ N_{summer} + 0.615\ C$	0.410	0.400	41.75	1.63
DV_{autumn}	$V = -0.815 + 0.009\ P_{autumn} + 0.046\ T_{autumn} - 0.391\ W_{autumn} - 3.43\ N_{autumn} + 0.011\ E$	0.402	0.390	32.17	2.31
DV_{winter}	$V = -0.405 + 0.016\ P_{winter} - 0.351\ W_{winter} - 0.003\ H + 0.028\ E - 0.049\ R$	0.455	0.444	39.92	1.61
SV_{day}	$V = -0.611 + 0.059\ T_{summer} - 0.054\ T_{winter} - 0.248\ W_{summer} + 0.29\ W_{winter} - 2.159 N_{winter} + 0.009\ E + 0.297\ C$	0.445	0.428	27.11	1.66
SV_{night}	$V = 0.028 + 0.006\ P_{winter} - 0.093\ W_{winter} - 0.006\ H + 2.5\ N_{summer} + 0.012\ E + 0.204\ C$	0.474	0.461	35.80	1.90

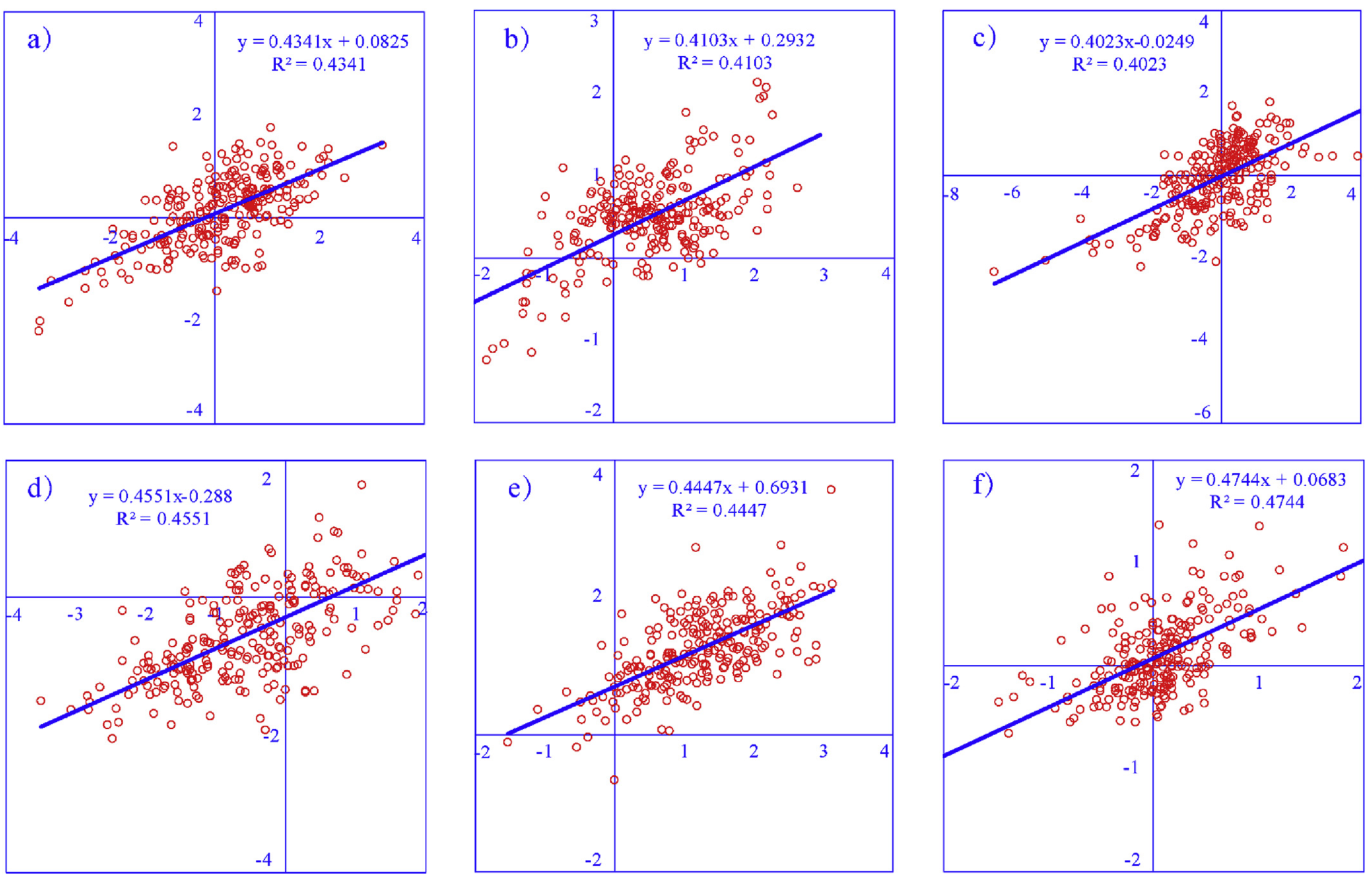

Fig. 5. Relationships between remotely-sensed and model-predicted variability of urban heat islands in 245 Chinese cities. Correlations of remotely-sensed and regression model-predicted day-night variability in spring (a), summer (b), autumn (c), and winter (d). Correlations of summer-winter variability in the daytime (e) and nighttime (f). Blue lines show the linear regression fitted to the data. The parameter bounds for the regression slope are at the 95% confidence interval. (For interpretation of the references to colour in this figure legend, the reader is referred to the Web version of this article.)

emissions. For example, the quantity of vehicles increased the DV in summer, while energy consumption contributed to the DV in autumn and winter. These two factors can affect the SV during both daytime and nighttime. Previous studies confirmed the important role of the background climate in explaining spatial–temporal variation in the UHI intensity (Miles and Esau, 2017). Another study showed that urbanization-induced vegetation loss significantly affected the summer UHIs (Yao et al., 2018). Our results showed that the indicator of urban area was not significant at explaining the DV and SV. This result was also coherent when comparing the UHI intensity during the rapid urbanization from 2002 to 2012. These findings were supported by those of previous reports showing that the impact of urban size and population on UHIs remained unclear and was likely to be region-specific (Peng et al., 2012; Yao et al., 2018).

4.2. Limitations of this study

This study focused on the impacts of local background climate and urbanization on VUHIs. It is important to note that several factors should be investigated in future studies. First, the urban morphology should be quantified from the horizontal and vertical dimensions to correlate with VUHIs. The urban morphology can affect the surface albedo and thus the acceptance of solar radiation (Alavipanah et al., 2018). Moreover, the urban morphology may influence the wind direction and velocity in urban regions (Hsieh and Huang, 2016). Second, the impact of air pollution on VUHIs should be focused on in the future. Climate warming and air pollution have been reported to be closely interwoven at the national and global scales (Cao et al., 2016a; IPCC, 2014; Li et al., 2016). A previous study showed that over the last decade in China, the

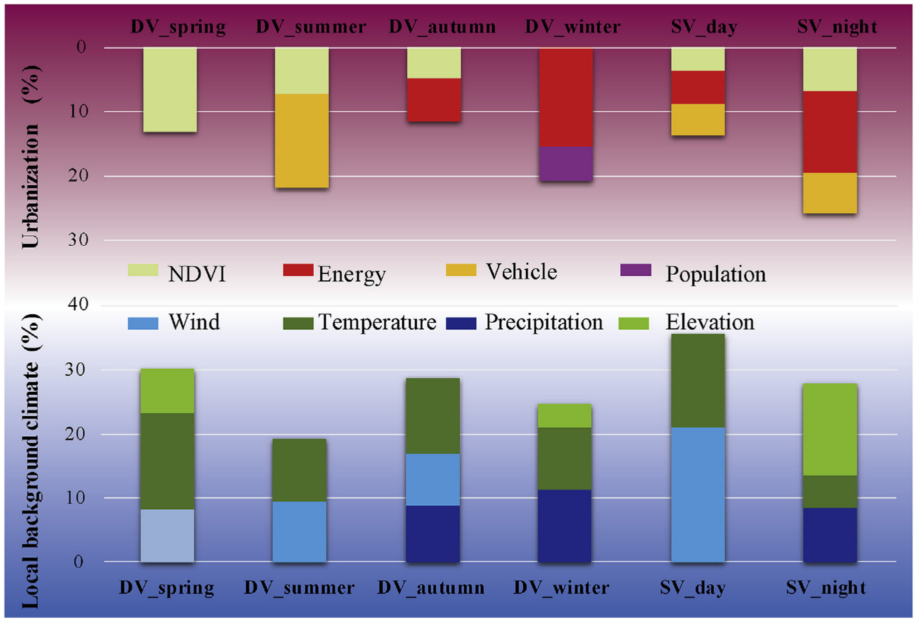

Fig. 6. Contributions of local background climate and urbanization to variability of urban heat islands in 245 Chinese cities. Local background climate was assessed using precipitation, air temperature, wind velocity, and the urban-rural difference in elevation. Urbanization was compared using urban green spaces and anthropogenic heat emissions (i.e., urban population, energy consumption, and quantity of vehicles). Contributions were quantified through stepwise multivariate regression of the day-night variability (DV) in spring, summer, autumn, and winter, and summer-winter variability (SV) in the daytime and nighttime. (For interpretation of the references to colour in this figure legend, the reader is referred to the Web version of this article.)

contribution of fossil-fuel CO_2 to climate change has become greater than that from land-use change (Li et al., 2016). A more recent study showed that urban heat islands can be affected by fine particles in urban regions (Wu et al., 2017). Accordingly, more detailed air pollutant data would be useful to predication of VUHIs. Third, the structure of urban energy consumption also influenced VUHIs predication. The anthropogenic heat emission was determined by not only the amount of energy, but also the composition of energy consumption (Ji and Chen, 2017; Sun et al., 2018). Further efforts on energy inventory should be made to quantify the correlation of anthropogenic heat and VUHIs at different times. In addition to the key factors revealed in the present study, the results indicate that detailed monitoring and the modelling of air pollution and warming are urgently needed to enable the development of effective adaptation policies. Finally, data processes methods and regression models should be improved in further studies. The urban boundaries and land surface temperatures retrieved from remote sensing images were not validated by in situ observations in the present study. Nevertheless, this study aimed to develop a feasible and practicable model based on limited factors for comparison of VUHIs among multiple cities. To accomplish this, we combined the effects of local background climate and urbanization in a linear formula to create a regression model. Further research regarding the nonlinear relationships among these factors would help improve the scientific basis of the model.

4.3. Implications for urban climate adaptation

Our demonstration of climate-induced VUHIs strongly suggests the need to include VUHIs in planning for future climate-change adaptation. The significant influences of climate background on VUHIs indicate that urban climate research and adaptation should not be conducted only in megacities as defined by urban size and population but should also consider local background climate (Lee and Kim, 2016; Nordio et al., 2015). Local “climate-smart” strategies for specific regions suggest it is necessary to identify geographically appropriate strategies for climate change adaptation (Georgescu et al., 2014). Furthermore, strategies of urban climate adaptation should be adjusted in relation to green spaces and anthropogenic sources of heat. When compared to “hard infrastructure” solutions, urban green spaces have the merits of flexibility and cost-effectiveness for reducing vulnerability under climate change while providing other important ecosystem services such as water conservation, recreation, and air quality improvement (Ellison et al., 2017; Gaffin et al., 2012; Gunawardena et al., 2017; Jones et al., 2012; Zhao et al., 2014; Zhou et al., 2014). Since daytime UHIs are regulated by evaporative cooling and shading of vegetation while nighttime UHIs are affected by more complex factors, the climate-mitigation effect of green spaces may be overrated and should be reevaluated according to different time periods (Naudts et al., 2016). Our study showing more frequent nighttime UHIs in the 245 cities with broad geographical distribution indicates that current greenspace-oriented adaptation approaches may not meet expectations, and that they may amplify VUHIs in certain seasons. In contrast, energy consumption has been recognized as a major factor contributing to winter warming (Zhang et al., 2013). Our results also revealed the critical roles that energy consumption and vehicle quantities play in VUHIs.

Climate change adaptation is among the biggest challenges China faces (Sun et al., 2014). At the 2015 UN Conference on Climate Change, China pledged to peak CO_2 emissions by around 2030. One of the important strategies to achieve this goal is raising the proportion of non-fossil fuels used during primary energy consumption. By 2030, urban areas will account for 83% of China's energy demand and 85% of its energy-related greenhouse gas emissions (Dhakal, 2009), and most of China's energy-intensive cities are of small or moderate size and largely located in the northeastern and western regions (Zhao et al., 2018). Therefore, city-specific energy-consumption control measures will benefit both the control of carbon emissions and adaptation to UHI variability. Different on- and off-peak price rates may promote the rational use of energy and enhance the adaptation of UHI variability. This large-scale

study of UHI variability and periodicity may have global implications for future climate adaptation in urban regions elsewhere. Attention should be paid to relating urban climate variability to global climate patterns to effectively link urban planning with sustainable global adaptation policies. We emphasize anthropogenic heat emissions as an important contributor to temperature variability and caution against the use of green spaces to mitigate urban warming. To put our results in perspective, more detailed observations of urban climates in specific regions and seasons are needed to improve decision-making.

5. Conclusions

This study investigated the diurnal and seasonal variability of urban heat islands (VUHIs) in 245 Chinese cities. The VUHIs from 2002 to 2012 had obvious periodicity in different years while significant diurnal and seasonal variability. The average diurnal VUHI is positive in summer but negative in other seasons. The underlying factors of local background climate and urbanization were quantified by regression models. The results revealed that a hot and humid climate amplify VUHIs while strong wind can mitigate them. The VUHIs were also affected by urbanization factors, including urban green spaces, vehicles, and energy consumption. Based on the key factors revealed in our study, the urban climate adaptation should be improved by developing local “climate-smart” strategies, anthropogenic heat reduction, and rational use of green planning for sustainable urban development. Notably, other factors of air pollution, urban morphology, and energy structures can influence VUHIs and should therefore be quantified in further studies. Although the present study might be enhanced by supplementation with more detailed data, these results expand our scientific understanding of the drivers of VUHIs. This study provides useful implications for identifying priority areas of urban climate adaptation and generates appropriate strategies for mitigating potential risks of urban climate variability.

Acknowledgments

We thank Dr. B. Jiang for providing technological supports to extract the urban and rural boundaries. The work was financed by the National Natural Science Foundation of China (grant 41471150).

Appendix A. Supplementary data

Supplementary data to this article can be found online at https://doi.org/10.1016/j.jclepro.2018.10.178.

References

Alavipanah, S., Schreyer, J., Haase, D., Lakes, T., Qureshi, S., 2018. The effect of multi-dimensional indicators on urban thermal conditions. J. Clean. Prod. 177, 115–123.
Cao, C., Lee, X., Liu, S., Schultz, N., Xiao, W., Zhang, M., Zhao, L., 2016a. Urban heat islands in China enhanced by haze pollution. Nat. Commun. 7, 12509.
Cao, Q., Yu, D.Y., Georgescu, M., Wu, J.G., 2016b. Impacts of urbanization on summer climate in China: an assessment with coupled land-atmospheric modeling. J. Geophys. Res. Atmos. 121, 10505–10521.
Clinton, N., Gong, P., 2013. MODIS detected surface urban heat islands and sinks: global locations and controls. Remote Sens. Environ. 134, 294–304.
Dhakal, S., 2009. Urban energy use and carbon emissions from cities in China and policy implications. Energy Pol. 37, 4208–4219.
Ellison, D., Morris, C.E., Locatelli, B., Sheil, D., Cohen, J., Murdiyarso, D., Gutierrez, V., van Noordwijk, M., Creed, I.F., Pokorny, J., Gaveau, D., Spracklen, D.V., Tobella, A.B., Ilstedt, U., Teuling, A.J., Gebrehiwot, S.G., Sands, D.C., Muys, B., Verbist, B., Springgay, E., Sugandi, Y., Sullivan, C.A., 2017. Trees, forests and water: cool insights for a hot world. Global Environ. Change 43, 51–61.
Estoque, R.C., Murayama, Y., Myint, S.W., 2017. Effects of landscape composition and pattern on land surface temperature: an urban heat island study in the megacities of Southeast Asia. Sci. Total Environ. 577, 349–359.
Fischer, E.M., Knutti, R., 2015. Anthropogenic contribution to global occurrence of heavy-precipitation and high-temperature extremes. Nat. Clim. Change 5, 560–564.
Fischer, E.M., Schar, C., 2010. Consistent geographical patterns of changes in high-impact European heatwaves. Nat. Geosci. 3, 398–403.
Gaffin, S.R., Rosenzweig, C., Kong, A.Y.Y., 2012. Adapting to climate change through urban green infrastructure. Nat. Clim. Change 2, 704-704.
Georgescu, M., Morefield, P.E., Bierwagen, B.G., Weaver, C.P., 2014. Urban adaptation can roll back warming of emerging megapolitan regions. Proc. Natl. Acad. Sci. U.S.A. 111, 2909–2914.
Gunawardena, K.R., Wells, M.J., Kershaw, T., 2017. Utilising green and bluespace to mitigate urban heat island intensity. Sci. Total Environ. 584, 1040–1055.
Hsieh, C.-M., Huang, H.-C., 2016. Mitigating urban heat islands: a method to identify potential wind corridor for cooling and ventilation. Comput. Environ. Urban. 57, 130–143.
Huang, C., Townshend, J.R.G., 2003. A stepwise regression tree for nonlinear approximation: applications to estimating subpixel land cover. Int. J. Rem. Sens. 24, 75–90.
Huang, T., Uchihama, D., Ochi, S., Yasuoka, Y., 2006. Assessment with satellite data of the urban heat island effects in Asian mega cities. Int. J. Appl. Earth Obs. 8, 34–48.
Imhoff, M.L., Zhang, P., Wolfe, R.E., Bounoua, L., 2010. Remote sensing of the urban heat island effect across biomes in the continental USA. Remote Sens. Environ. 114, 504–513.
IPCC, 2014. Climate change 2014: synthesis report. In: Team, C.W., Pachauri, R.K., Meyer, L.A. (Eds.), Contribution of Working Groups I, II and III to the Fifth Assessment Report of the Intergovernmental Panel on Climate Change. IPCC, Geneva, Switzerland.
Ji, X., Chen, B., 2017. Assessing the energy-saving effect of urbanization in China based on stochastic impacts by regression on population, affluence and technology (STIRPAT) model. J. Clean. Prod. 163, S306–S314.
Jiang, B., Yin, J.J., Liu, Q.L., 2015. Zipf's law for all the natural cities around the world. Int. J. Geogr. Inf. Sci. 29, 498–522.
Jones, H.P., Hole, D.G., Zavaleta, E.S., 2012. Harnessing nature to help people adapt to climate change. Nat. Clim. Change 2, 504–509.
Kolasa-Wiecek, A., 2015. Stepwise multiple regression method of greenhouse gas emission modeling in the energy sector in Poland. J. Environ. Sci. China 30, 47–54.
Lee, J.Y., Kim, H., 2016. Projection of future temperature-related mortality due to climate and demographic changes. Environ. Int. 94, 489–494.
Li, B.G., Gasser, T., Ciais, P., Piao, S.L., Tao, S., Balkanski, Y., Hauglustaine, D., Boisier, J.P., Chen, Z., Huang, M.T., Li, L.Z., Li, Y., Liu, H.Y., Liu, J.F., Peng, S.S., Shen, Z.H., Sun, Z.Z., Wang, R., Wang, T., Yin, G.D., Yin, Y., Zeng, H., Zeng, Z.Z., Zhou, F., 2016. The contribution of China's emissions to global climate forcing. Nature 531, 357–361.
Li, W.F., Cao, Q.W., Lang, K., Wu, J.S., 2017a. Linking potential heat source and sink to urban heat island: heterogeneous effects of landscape pattern on land surface temperature. Sci. Total Environ. 586, 457–465.
Li, X., Zhou, Y., Asrar, G.R., Mao, J., Li, X., Li, W., 2017b. Response of vegetation phenology to urbanization in the conterminous United States. Global Change Biol. 23, 2818–2830.
Miles, V., Esau, I., 2017. Seasonal and spatial characteristics of urban heat islands (UHIs) in northern west siberian cities. Rem. Sens. 9, 15.
Naudts, K., Chen, Y., McGrath, M., Ryder, J., 2016. Europe's forest management did not mitigate climate warming. Science 351, 597–600.
Nordio, F., Zanobetti, A., Colicino, E., Kloog, I., Schwartz, J., 2015. Changing patterns of the temperature-mortality association by time and location in the US, and implications for climate change. Environ. Int. 81, 80–86.
Parker, D.E., 2004. Large-scale warming is not urban. Nature 432, 290.
Patz, J.A., Campbell-Lendrum, D., Holloway, T., Foley, J.A., 2005. Impact of regional climate change on human health. Nature 438, 310–317.
Peng, J., Xie, P., Liu, Y.X., Ma, J., 2016. Urban thermal environment dynamics and associated landscape pattern factors: a case study in the Beijing metropolitan region. Remote Sens. Environ. 173, 145–155.
Peng, S., Piao, S., Ciais, P., Friedlingstein, P., Ottle, C., Breon, F.M., Nan, H., Zhou, L., Myneni, R.B., 2012. Surface urban heat island across 419 global big cities. Environ. Sci. Technol. 46, 696–703.
Ramamurthy, P., Bou-Zeid, E., 2017. Heatwaves and urban heat islands: a comparative analysis of multiple cities. J. Geophys. Res. Atmos. 122, 168–178.
Sailor, D.J., Georgescu, M., Milne, J.M., Hart, M.A., 2015. Development of a national anthropogenic heating database with an extrapolation for international cities. Atmos. Environ. 118, 7–18.
Schwarz, N., Lautenbach, S., Seppelt, R., 2011. Exploring indicators for quantifying surface urban heat islands of European cities with MODIS land surface temperatures. Remote Sens. Environ. 115, 3175–3186.
Steeneveld, G.J., Koopmans, S., Heusinkveld, B.G., Theeuwes, N.E., 2014. Refreshing the role of open water surfaces on mitigating the maximum urban heat island effect. Landsc. Urban Plann. 121, 92–96.
Stone, B., Vargo, J., Liu, P., Hu, Y.T., Russell, A., 2013. Climate change adaptation through urban heat management in Atlanta, Georgia. Environ. Sci. Technol. 47, 7780–7786.
Sun, R.H., Wang, Y.N., Chen, L.D., 2018. A distributed model for quantifying temporal-spatial patterns of anthropogenic heat based on energy consumption. J. Clean. Prod. 170, 601–609.
Sun, Y., Zhang, X., Zwiers, F., Song, L., Wan, H., Hu, T., Yin, H., Ren, G., 2014. Rapid increase in the risk of extreme summer heat in Eastern China. Nat. Clim. Change

4, 1082–1085.

Sun, Y., Zhang, X.B., Ren, G.Y., Zwiers, F.W., Hu, T., 2016. Contribution of urbanization to warming in China. Nat. Clim. Change 6, 706–709.

Theodosiou, G., Stylos, N., Koroneos, C., 2015. Integration of the environmental management aspect in the optimization of the design and planning of energy systems. J. Clean. Prod. 106, 576–593.

UNDESA, 2015. (United nations, department of economic and social affairs, population division). World population prospects: the 2015 revision. In: Cohen, B., Pelletier, F., al, e. (Eds.), Methodology of the United Nations Population Estimates and Projections. No. ESA/P/WP, p. 242.

Wang, J., Huang, B., Fu, D., Atkinson, P., 2015. Spatiotemporal variation in surface urban heat island intensity and associated determinants across major Chinese cities. Rem. Sens. 7, 3670.

Wu, H., Wang, T., Riemer, N., Chen, P., Li, M., Li, S., 2017. Urban heat island impacted by fine particles in Nanjing, China. Sci. Rep. 7.

Yamashita, T., Yamashita, K., Kamimura, R., 2007. A stepwise AIC method for variable selection in linear regression. Commun. Stat. Theor. M. 36, 2395–2403.

Yao, R., Wang, L.C., Huang, X., Zhang, W.W., Li, J.L., Niu, Z.G., 2018. Interannual variations in surface urban heat island intensity and associated drivers in China. J. Environ. Manag. 222, 86–94.

Youngsteadt, E., Ernst, A.F., Dunn, R.R., Frank, S.D., 2017. Responses of arthropod populations to warming depend on latitude: evidence from urban heat islands. Global Change Biol. 23, 1436–1447.

Yu, Z.W., Xu, S.B., Zhang, Y.H., Jorgensen, G., Vejre, H., 2018. Strong contributions of local background climate to the cooling effect of urban green vegetation. Sci. Rep. 8, 9.

Zhang, G.J., Cai, M., Hu, A.X., 2013. Energy consumption and the unexplained winter warming over northern Asia and North America. Nat. Clim. Change 3, 466–470.

Zhao, J., Chen, Y., Ji, G., Wang, Z., 2018. Residential carbon dioxide emissions at the urban scale for county-level cities in China: a comparative study of nighttime light data. J. Clean. Prod. 180, 198–209.

Zhao, L., Lee, X., Smith, R.B., Oleson, K., 2014. Strong contributions of local background climate to urban heat islands. Nature 511, 216–219.

Zhao, S., Liu, S., Zhou, D., 2016. Prevalent vegetation growth enhancement in urban environment. Proc. Natl. Acad. Sci. U.S.A. 113, 6313–6318.

Zhou, D., Zhang, L., Li, D., Huang, D., Zhu, C., 2016. Climate-vegetation control on the diurnal and seasonal variations of surface urban heat islands in China. Environ. Res. Lett. 11, 11.

Zhou, D., Zhao, S., Liu, S., Zhang, L., Zhu, C., 2014. Surface urban heat island in China's 32 major cities: spatial patterns and drivers. Remote Sens. Environ. 152, 51–61.

Zhou, D., Zhao, S., Zhang, L., Sun, G., Liu, Y., 2015. The footprint of urban heat island effect in China. Sci. Rep. 5, 11160.

Zhou, L., Dickinson, R.E., Tian, Y., Fang, J., Li, Q., Kaufmann, R.K., Tucker, C.J., Myneni, R.B., 2004. Evidence for a significant urbanization effect on climate in China. Proc. Natl. Acad. Sci. U.S.A. 101, 9540–9544.